

Effect of Temperature on Thermogalvanic Coupling of Alloy 31 in LiBr Solutions Studied by Means of Imposed Potential Measurements

R.M. Fernández-Domene, E. Blasco-Tamarit, D.M. García-García, J. García-Antón *

Ingeniería Electroquímica y Corrosión (IEC). Departamento de Ingeniería Química y Nuclear. ETSI Industriales. Universidad Politécnica de Valencia. P.O. Box 22012, E-46071 Valencia. Spain.

*E-mail: jgarciaa@iqn.upv.es

Received: 13 May 2011 / Accepted: 2 July 2011 / Published: 1 August 2011

Corrosion resistance of Alloy 31, a highly alloyed stainless steel (UNS N08031) were studied in heavy brine LiBr solutions (400, 700 and 992 g/l) at different temperatures using electrochemical techniques. The mixed potential theory was used to evaluate thermogalvanic corrosion of Alloy 31 in the studied LiBr solutions. Potentiodynamic curves indicate that high temperatures favoured both cathodic and anodic processes, increasing passive current densities and decreasing the pitting potential. Generally, the cold electrode of the pair was the anode of the thermogalvanic cell.

Keywords: Stainless steel, passive film, temperature, thermogalvanic corrosion.

1. INTRODUCTION

Lithium bromide (LiBr) solutions are widely used as a refrigerant for absorption-type air-conditioning and industrial drying systems due to its good thermodynamic properties [1-4]. However, these LiBr solutions can cause serious corrosion problems on the metallic components in absorption plants [5-13]. The development of corrosion resistant metallic materials, such as Alloy 31, has become one of the key issues in new absorption systems. Alloy 31 is a highly alloyed austenitic stainless steel (UNS N08031), with 26.75% Cr, 31.85% Ni and 6.60% Mo which is characterised by its high resistance to corrosion in halide media [10-12].

When a material in a corrosive environment is subjected to a temperature gradient, a potential difference between the hot and cold zones may arise, what is known as thermogalvanic corrosion. Hence, process equipment surfaces exposed to service environments and subjected to large temperature gradients will undergo rapid deterioration. The anodic properties of the material depend

on the temperature, as well as the properties of the environment along the metal surface. Often this affects the cathodic reaction, which should also be taken into account when such a corrosion form is analysed.

The aim of this work was to evaluate the effect of temperature on the electrochemical behaviour of Alloy 31 in three heavy brine LiBr solutions (400, 700 and 992 g/l). From the potentiodynamic polarization curves (imposed potential measurements), the mixed potential theory was applied in order to study thermogalvanic corrosion between Alloy 31 electrodes subjected to different temperatures.

2. EXPERIMENTAL PROCEDURE

2.1. Materials and specimen preparation

The material tested was the highly alloyed austenitic stainless steel Alloy 31 (UNS N08031: 26.75% Cr, 31.85% Ni, 1.50% Mn, 0.10% Si, 6.60% Mo, 1.21% Cu, 31.43% Fe, 0.002% S, 0.017% P, 0.005% C, 0.193% N), provided by ThyssenKrupp VDM. Alloy 31 electrodes were cylindrically shaped (8-mm diameter and 55 mm long) and covered with a polytetrafluoroethylene (PTFE) coating. The exposed area to the solution was 0.5 cm². All specimens were wet abraded from 500 SiC (silicon carbide) grit to 4000 SiC grit, and finally rinsed with distilled water.

The samples were tested in 400 g/l (4.61 M), 700 g/l (8.06 M) and 992 g/l (11.42 M) LiBr solutions, prepared from LiBr (98 wt.%), from PANREAC.

2.2. Potentiodynamic tests

Potentiodynamic polarisation curves were determined by using an Autolab PGSTAT302N potentiostat. The experimental arrangement consists of two parts: a horizontal electrochemical cell [14,15] with the data acquisition equipment and an image acquisition unit formed by a trinocular microscope-stereoscope (NIKON SMZ-U) zoom 1:10 and a colour video camera (SONY SSC-C370P). The image acquisition unit allows observing the electrode surface in real-time during potentiodynamic polarization and to relate the events that take place on the electrode surface to the polarization curve.

The potentials of the working electrode were measured against a silver-silver chloride (Ag/AgCl 3M KCl) reference electrode. The auxiliary electrode was a platinum (Pt) wire. LiBr solutions were deaerated by bubbling N₂ before and during the tests over the electrolyte. Potentiodynamic curves were performed in the three LiBr solutions mentioned above (namely, 400, 700 and 992 g/l LiBr), at four different temperatures (25, 50, 75 and 100° C; in the 400 g/l LiBr solution, the maximum temperature was 75° C, since at 100° C the solution showed signs of boiling). Before each polarisation, the sample was immersed in the test solution for 1h at the open circuit potential (OCP). The average value of the potentials recorded during the last 300 s was the value of the OCP (ASTM G-5 [16]). After the OCP test, the specimen potential was scanned from a potential value

of $-150 \text{ mV}_{\text{Ag}/\text{AgCl}}$ with respect to the OCP value towards the active direction at 0.1667 mV/s . Corrosion current density (i_{corr}) and corrosion potential (E_{corr}) were estimated from these curves; information about the general electrochemical behaviour of the materials was obtained. The thermogalvanic corrosion generated by the electrical contact between the Alloy 31 electrodes subjected to different temperature gradients was also estimated from these polarisation curves according to the mixed potential method. The thermogalvanic current density (i_{th}) and the mixed potential (E_M) of the pair were obtained.

3. RESULTS AND DISCUSSION

3.1. Potentiodynamic tests

In all the tests, open circuit potential measurements were very stable. At all temperatures and LiBr solutions under study, the open circuit potential value shifted toward less negative potentials immediately after immersion. Moreover, using the patented image acquisition unit [14,15], no change was observed on the electrode surface during the hour of the OCP test. Both facts indicate the good properties of the passive film formed on Alloy 31 surface [6,10-12,17-20]. The ennoblement of the OCP value could be attributable to healing of the pre-immersion air formed oxide film and further thickening of this film as a result of the interaction between the electrolyte and the metal surface [19]. The growth of the oxide film will continue until the film reaches a stable thickness.

The OCP values of Alloy 31 in the 400, 700 and 992 g/l LiBr solutions at different temperatures are shown in Table 1. It can be seen that OCP values shifted towards more positive values as temperature increased.

Table 1. OCP values for Alloy 31 in the studied LiBr solutions at different temperatures.

	25° C	50° C	75° C	100° C
OCP ($\text{mV}_{\text{Ag}/\text{AgCl}}$)				
400 g/l LiBr	-374 ± 12	-327 ± 6	-271 ± 17	-----
700 g/l LiBr	-298 ± 24	-286 ± 13	-133 ± 8	-26 ± 4
992 g/l LiBr	-248 ± 8	-247 ± 37	-104 ± 1	-96 ± 6

Potentiodynamic polarisation curves for Alloy 31 in the three LiBr solutions at different temperatures are presented in Figure 1. In general, cathodic current densities increased with temperature. In previous works in LiBr media [6,10,12,20,21], an increase in cathodic current densities to higher values with temperature was also observed. This increase of cathodic current densities as temperature increases could be expected if the cathodic reaction were, at least partially, controlled by diffusion, since a limiting current density is not observed. Temperature enhances mass transfer to or from the metallic surface, increasing the cathodic reaction rate [12,21].

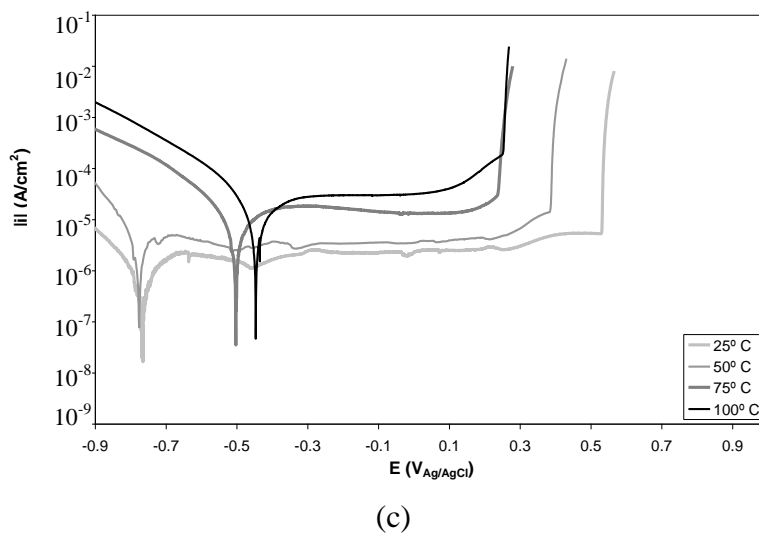
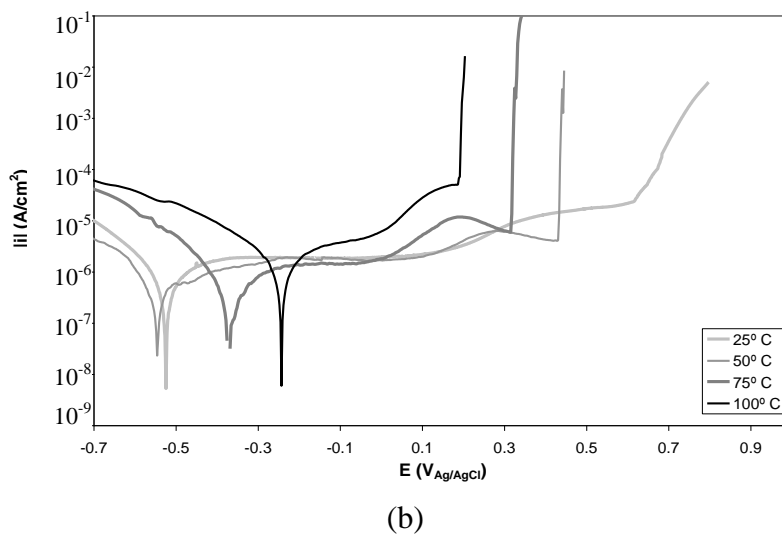
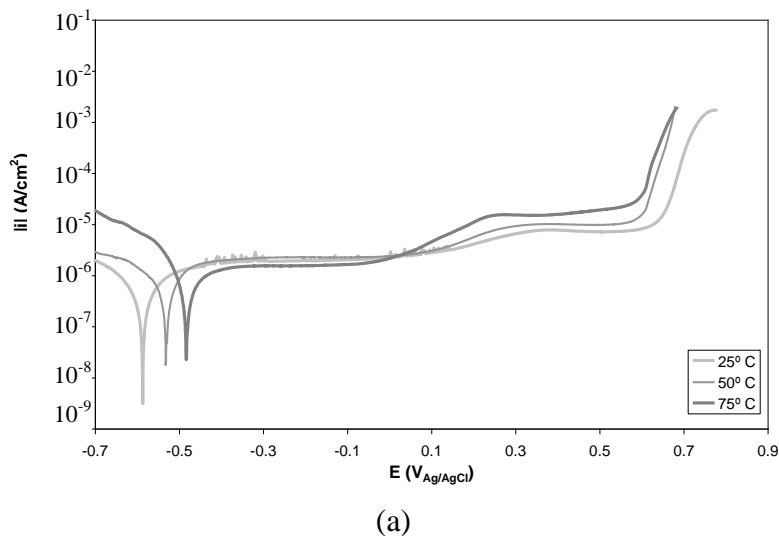


Figure 1. Potentiodynamic polarization curves for Alloy 31 at different temperatures for (a) 400 g/l LiBr, (b) 700 g/l LiBr and (c) 992 g/l LiBr solutions.

From the potentiodynamic polarisation curves, corrosion potentials (E_{corr}) and corrosion current densities (i_{corr}) were obtained (Table 2). It can be observed that E_{corr} shifted towards more positive values and i_{corr} values increased with temperature. This increase in corrosion potential and corrosion current density seems to be related to the increase in cathodic current densities and, consequently, to the enhancement of the cathodic reaction with temperature [6,10,12,21,22]. For the tests performed at 50° C in the 700 and 992 g/l LiBr solutions, E_{corr} did not increase with temperature, but shifted slightly towards more negative values. This fact could be explained because temperature affects not only the cathodic branch of the potentiodynamic curve but also the anodic one. Thus, at 50° C in the 700 and 992 g/l LiBr solutions, temperature had more influence on the anodic branch than on the cathodic branch, shifting the corrosion potential, E_{corr} , towards more negative potentials.

Table 2. Electrochemical parameters for Alloy 31 in the studied LiBr solutions at different temperatures.

C_{LiBr} (g/l)	T (°C)	E_{corr} (mV)	i_{corr} ($\mu\text{A}/\text{cm}^2$)	i_p ($\mu\text{A}/\text{cm}^2$)	E_p (mV)	$E_p - E_{corr}$ (mV)
400	25	-560 ± 37	0.52 ± 0.03	3.21 ± 0.29	685 ± 1	1245 ± 38
	50	-533 ± 29	0.59 ± 0.04	5.05 ± 0.78	643 ± 9	1176 ± 38
	75	-428 ± 78	0.77 ± 0.07	5.81 ± 0.93	622 ± 5	1050 ± 83
700	25	-492 ± 45	0.62 ± 0.03	3.85 ± 1.40	664 ± 15	1156 ± 60
	50	-527 ± 23	0.68 ± 0.07	3.98 ± 0.31	434 ± 28	961 ± 51
	75	-375 ± 41	1.05 ± 0.04	4.36 ± 0.77	323 ± 23	698 ± 64
	100	-243 ± 33	1.84 ± 0.10	11.06 ± 2.10	197 ± 21	440 ± 54
992	25	-770 ± 5	0.75 ± 0.01	2.36 ± 0.09	533 ± 11	1303 ± 16
	50	-772 ± 5	2.86 ± 0.8	3.81 ± 0.92	385 ± 26	1157 ± 31
	75	-496 ± 23	5.76 ± 0.8	9.51 ± 1.72	239 ± 6	735 ± 29
	100	-447 ± 32	9.82 ± 0.5	14.65 ± 3.04	196 ± 8	643 ± 40

Alloy 31 passivated in the three LiBr solutions at all temperatures, since a range where current density values were constant is clearly observed in all polarisation curves (Figure 1). Alloy 31 registered an approximately stable current density value (passive current density, i_p) within this passive range, although a peak can be discerned in most of the curves before the increase in current density due to pitting. This peak can be related to the transpassive dissolution of Cr-containing species and is closely related to the passive film breakdown and localised corrosion phenomena [12]. Apart from this peak, current density transients scarcely appeared along the potentiodynamic curves at any LiBr concentration and temperature, indicating an absence of metastable pitting and high stability of the passive film even at 100° C.

However, the obtained results show that the properties of the passive film formed under potential imposition degraded with temperature, since the higher the solution temperature, the higher the passive current density values (i_p) and the narrower the passive range ($E_p - E_{corr}$) (Table 2).

Moreover, pitting potential (E_p), which is the potential limit above which the formation of stable pitting begins and is defined in this work as the potential at which current density reaches $100 \mu\text{A}/\text{cm}^2$ [6,7,10,11], decreased with increasing temperature in the three LiBr solutions (Table 2). Consequently, it can be said that Alloy 31 is less corrosion resistant as temperature increases, in the three LiBr solutions under study. These results reveal that the passive films formed at lower temperatures are significantly less defective and more resistant to film breakdown than those formed at higher temperatures, as reported by several authors [6,10,12,17-26].

By way of illustration, Figure 2 shows images of the Alloy 31 surface at different points of the polarization curve in the 700 g/l LiBr solution at 50°C .

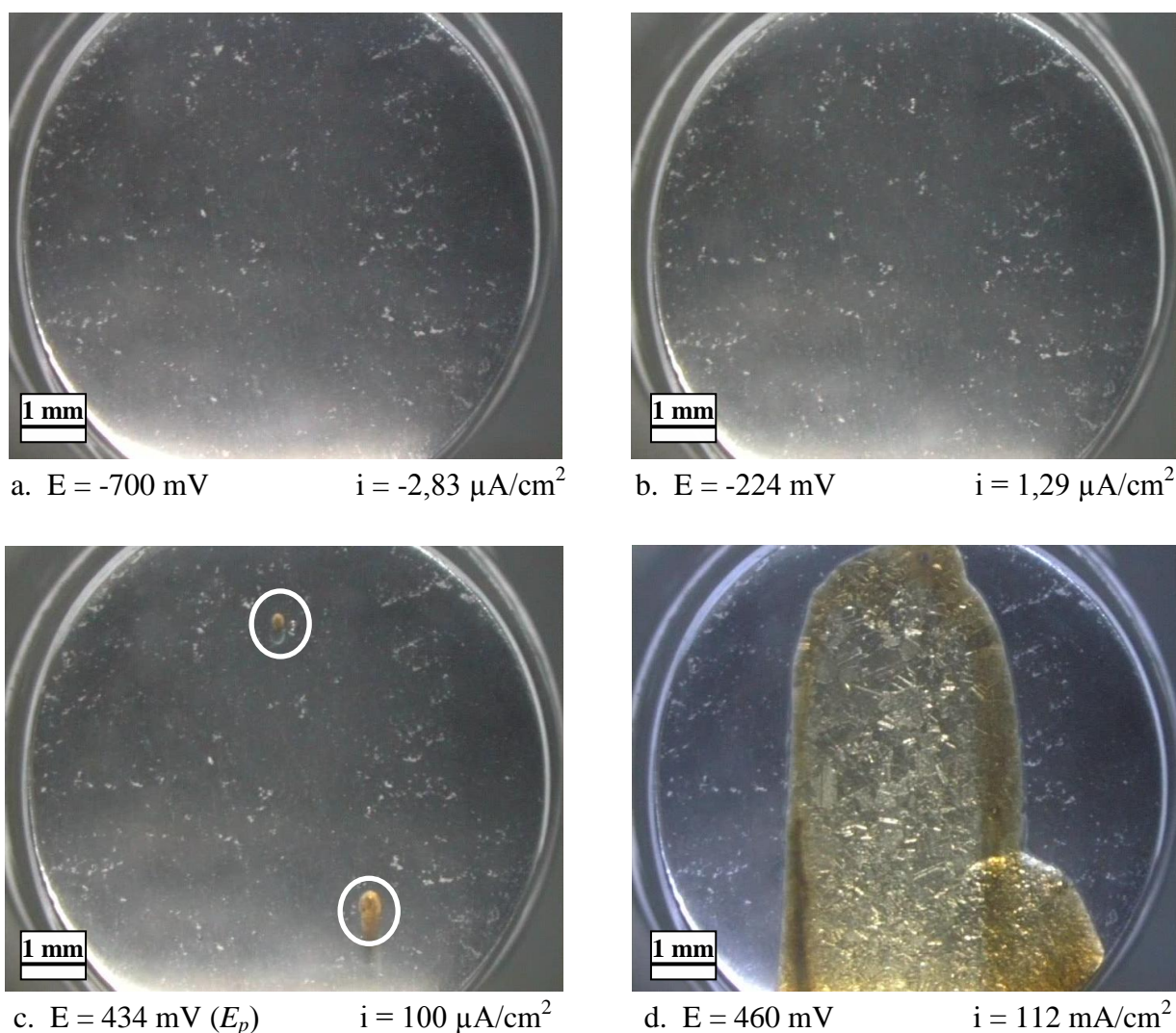


Figure 2. images of the Alloy 31 surface at different points of the polarization curve in the 700 g/l LiBr solution at 50°C

These images were taken in situ by using the patented image acquisition unit [14,15]. It can be observed that the electrode surface did not suffer any damage at potentials within the passive region (Figure 2b). Figure 2c corresponds to pitting potential (E_p) of Alloy 31 in the 700 g/l LiBr solution at

50° C, and shows the appearance of the first stable pits formed on the electrode surface, which imply the onset of pitting corrosion. Figure 2d corresponds to the end of the test, where the highest current density value was reached. It can be seen that at the end of the test, the damage was spread over a wide area of the electrode surface, since new pits nucleated and grew fast. Moreover, the corrosion products generated at localized sites changed the conditions around them and, and catalyzed the corrosion phenomenon. Thus, it can be said that corrosion began at localized sites of the surface and continued through the paths formed by the corrosion products generated from the sites. Other authors have obtained similar results [10,11].

3.2. Thermogalvanic corrosion using imposed potential measurements

According to the mixed potential theory, the corrosion potentials of the two metals in the environment under consideration will determine the direction of the transfer of electrons, although they will provide no information on the rate of this electron transfer. When two pieces of the same metal M are immersed in an electrolyte and exposed to a temperature gradient, $\Delta T = T_2 - T_1$ (with $T_1 < T_2$), a potential different between both electrodes will arise. If $E_{corr,T1}$ is more positive than $E_{corr,T2}$ the transfer of electrons will be from M_{T2} to M_{T1} , that is, the thermogalvanic coupling of the two electrodes will lead to stimulation of the anodic reaction on the metal at T_2 (corrosion rate of M_{T2} will consequently increase compared with the rate when metals are uncoupled) and to the simultaneous cathodic protection of the electrode at T_1 (corrosion rate of M_{T1} will decrease compared with the rate when metals are uncoupled) [27,28].

Potentiodynamic polarisation curves shown in Figure 1 can be used to illustrate the effect of thermogalvanic coupling. It can be observed that the cold electrode was the anodic member of the pair in most of the experiments, since E_{corr} values were generally higher as temperature increased. The mixed potential of the pairs, E_M (determined as the potential where the cathodic branch of the nobler electrode intersects the anodic branch of the more active electrode), and thermogalvanic current densities (i_{th}) are gathered in Table 3. In these imposed potential measurements, minimal differences of 100-130 mV between the corrosion potential of the cathodic and the anodic member of the pair ($E_C - E_A$) are necessary to consider the galvanic (and thermogalvanic) effect relevant [29]. In the present study, thermogalvanic effect between the cold and hot Alloy 31 electrodes is important in all the LiBr solutions at 75 and 100° C, with $E_C - E_A$ values higher than 100 mV. However, due to the passive behaviour of Alloy 31, these potential differences do not involve high thermogalvanic current densities (Table 3). Nevertheless, in those cases where the cold electrode was the anode of the thermogalvanic pair, i_{th} was higher than i_{corr} at 25° C, which indicates that thermogalvanic coupling negatively affects the corrosion resistance of the cold anode. According to Mansfeld and Kendel [30], the relative increase in the corrosion rate of the anodic member of the pair could be expressed by the ratio i_{th}/i_{corr} , whose magnitude can be used as a guide that reflects the severity of the galvanic and thermogalvanic effect in a couple, and it was suggested that a value less than 5 implies compatibility of the members in the couple [29-31]. Thus, these results show that thermogalvanic effect was not severe, since current density values were rather small.

Table 3. Mixed potentials (E_M) and thermogalvanic current densities (i_{th}) for the pair cold Alloy 31 – hot Alloy 31 in the studied LiBr solutions using the mixed potential theory.

C_{LiBr} (g/l)	Test	$E_C - E_A$ (mV)	E_M (mV)	i_{th} ($\mu A/cm^2$)	Anode
400	25°C-50°C	27	-550 ± 33	0.53 ± 0.03	Cold electrode
	25°C-75°C	132	-507 ± 49	1.02 ± 0.05	Cold electrode
700	25°C-50°C	35	-533 ± 29	0.23 ± 0.04	Hot electrode
	25°C-75°C	117	-429 ± 43	0.92 ± 0.03	Cold electrode
	25°C-100°C	249	-280 ± 39	1.79 ± 0.06	Cold electrode
992	25°C-50°C	2	-773 ± 7	0.37 ± 0.06	Hot electrode
	25°C-75°C	274	-508 ± 14	1.54 ± 0.05	Cold electrode
	25°C-100°C	323	-443 ± 18	1.30 ± 0.3	Cold electrode

It can be concluded that, in general, an increase in temperature gradient favoured the anodic behaviour of the cold electrode, since the difference $E_C - E_A$ increased, making the thermogalvanic effect more severe. This fact could be attributable to an enhancement of the cathodic reaction as temperature increased.

4. CONCLUSIONS

In general, corrosion potentials (E_{corr}) shifted towards more positive values and corrosion current densities (i_{corr}) values increased with temperature, because of the enhancement of the cathodic reaction as temperature increased.

Passive current density (i_p) increased and the passive range, as well as pitting potential (E_p), decreased with temperature, suggesting a loss of protective properties of the passive film formed on Alloy 31 surface with increasing temperatures.

According to the mixed potential theory, the cold Alloy 31 electrode was the anode of the thermogalvanic couple in most cases, since temperature favoured the cathodic behaviour of the hot electrode.

An increase in temperature gradient favoured the anodic behaviour of the cold electrode, since the difference $E_C - E_A$ increased, making the thermogalvanic effect more severe.

ACKNOWLEDGEMENTS

We wish express our gratitude to the Ministerio de Ciencia e Innovación (Project CTQ2009-07518), for the economical support of this research, to Thyssen Krupp for supplying the materials, and to Dr. M. Asunción Jaime for her translation assistance.

References

1. S. Wu, I. W. Eames, *Appl. Energy* 66 (2000) 251-266.
2. American Society of Heating, Refrigerating and Air-Conditioning Engineers (ASHRAE) Handbook, *Absorption Cooling, Heating and Refrigeration Equipment (Refrigeration Volume)*, 2002.
3. P. Sriksirin, S. Aphornratana, S. Chungpaibulpatana, *Renew. Sust. Energ. Rev.* 5 (2001) 343-372.
4. K. E. Herold, R. Radermacher, S. Klein, *Absorption Chillers and Heat Pumps*, CRC Press, 1996.
5. M.T. Montañés, R. Sánchez-Tovar, J. García-Antón, V. Pérez-Herranz, *Int. J. Electrochem. Sci.* 5 (2010) 1934-1947.
6. R. Leiva-García, M.J. Muñoz-Portero, J. García-Antón, *Int. J. Electrochem. Sci.* 6 (2011) 442-460.
7. E. A. Abd El Meguid, N. K. Awad, *Corros. Sci.* 51 (2009) 1134-1139.
8. D.M. García-García, E. Blasco-Tamarit, J. García-Antón, *Int. J. Electrochem. Sci.* 6 (2011) 1237-1249.
9. D. Itzhak, O. Elias, *Corrosion* 50 (1994) 131-137.
10. E. Blasco-Tamarit, A. Igual-Muñoz, J. García-Antón, D. García-García, *Corros. Sci.* 50 (2008) 1848-1857.
11. R.M. Fernández-Domene, E. Blasco-Tamarit, D. M. García-García, J. García-Antón, *Corros. Sci.* 52 (2010) 3453-3464.
12. E. Blasco-Tamarit, D.M. García-García, J. García-Antón, *Corros. Sci.* 53 (2011) 784-795.
13. E. Sarmiento, J.G. González-Rodríguez, J. Uruchurtu, O. Sarmiento, M. Menchaca, *Int. J. Electrochem. Sci.* 4 (2009) 144-155.
14. J. García-Antón, A. Igual-Muñoz, J. L. Guiñón, V. Pérez-Herranz, Spain, P-200002525, 2000.
15. J. García-Antón, A. Igual-Muñoz, J. L. Guiñón, V. Pérez-Herranz, Spain, P-200002526, 2000.
16. ASTM G-5, *Test Method for Making Potentiostatic and Potentiodynamic Anodic Polarization Measurements*, American Society for Testing and Materials, 2004.
17. A. Igual-Muñoz, J. García-Antón, J.L. Guiñón, V. Pérez-Herranz, *Corros. Sci.* 48 (2006) 3349-3374.
18. Z.F. Wang, C.L. Briant, K.S. Kumar, *Corrosion* 55 (1999) 128-138.
19. E.A. Abd El Meguid, A.A. Abd El Latif, *Corros. Sci.* 49 (2007) 263-275.
20. R. Leiva-García, M.J. Muñoz-Portero, J. García-Antón, *Corros. Sci.* 52 (2010) 950-959.
21. R. Sánchez-Tovar, M.T. Montañés, J. García-Antón, *Corros. Sci.* 52 (2010) 722-733.
22. A. Neville, T. Hodgkiess, *Corros. Sci.* 38 (1996) 927-956.
23. C.T. Kwok, H.C. Man, L.K. Leung, *Wear* 211 (1997) 84-93.
24. J.J. Park, S.I. Pyun, S.B. Lee, *Electrochim. Acta* 49 (2004) 281-292.
25. R.M. Carranza, M.G. Alvarez, *Corros. Sci.* 38 (1996) 909-925.
26. K.J. Park, S.J. Ahn, H.S. Kwon, *Electrochim. Acta* 56 (2011) 1662-1669.
27. V. Ashworth, P.J. Boden, *Corros. Sci.* 14 (1974) 183-197.
28. M.J. Pryor, D.J. Astley, in: L.L. Shreir (Ed.), R.A. Jarman (Ed.), G.T. Burstein (Ed.), *Corrosion and Corrosion Control, vol. 1*, 3rd ed., Butterworth-Heinemann, Oxford, 1994, Ch. 1.7.
29. E. Blasco-Tamarit, A. Igual-Muñoz, J. García-Antón, D. García-García, *Corros. Sci.* 49 (2007) 1000-1026.
30. F. Mansfeld, J.V. Kendel, *Laboratory studies of galvanic corrosion of aluminium alloys*, in: R. Raboian (Ed.), W.D. France (Ed.), *Galvanic and Pitting Corrosion-Field and Laboratory Studies*, ASTM STP 576, ASTM, New York, 1976, pp. 20-47.
31. F.T. Cheng, K.H. Lo, H.C. Man, *Surf. Coat. Technol.* 172 (2003) 316-321.